A Solvothermal Route to High-Surface-Area Nanostructured MoS_2

Nicole Berntsen,[†] Tobias Gutjahr,[†] Lars Loeffler,[‡] John R. Gomm,[‡] Ram Seshadri,*[,‡] and Wolfgang Tremel*[,†]

Institut für Anorganische Chemie und Analytische Chemie, Johannes Gutenberg Universität, Mainz, Duesbergweg 10-14, Mainz D55099, Germany, and Materials Department and Materials Research Laboratory, University of California Santa Barbara, Santa Barbara California 93106-5050

Received August 7, 2003. Revised Manuscript Received September 8, 2003

We describe a simple route to nanostructured MoS_2 based on the decomposition of the cluster-based precursor $(NH_4)_2Mo_3S_{13}{\cdot}xH_2O$ in solvothermal toluene at 653 K. Solvothermal decomposition results in nanostructured material distinct from that obtained by decomposition of the precursor in sealed quartz tubes at the same temperature. When carried out in the presence of the surfactant cetyltrimethylammonium bromide (CTAB), the decomposition results in unusual string-like morphologies of highly disordered MoS_2 lamellae, with high surface areas. An attempt to understand representative sizes and structures of the nano-MoS_2 produced by the different methods has been made using DIFFaX simulations of the powder X-ray diffraction patterns.

Introduction

The layered structure of the early transition metal dichalcogenides MQ_2 easily lend themselves to the formation of a variety of nanostructures. A number of years ago, Divigalpitiya et al.[1] showed that MoS_2 can be separated sheet-by-sheet by a process of exfoliation, and then restacked with organic molecules to obtain interesting hybrid materials. The huge body of work on carbon nanostructures, particularly the discovery of carbon nanotubes[2] and carbon onions[3] encouraged Tenne and co-workers[4] to pursue related MQ_2-based, concentric, closed-shell materials, laying the foundation for an entire area of nanostructures based on layered inorganic materials.[5]

A characteristic feature of closed-shell MQ_2-derived structures is that they require high temperatures of preparation (∼1100 K) for the ends of single MQ_2 sheets to "knit" together through the formation of rhomboidal and triangular point defects which provide curvature to the otherwise flat MQ_2 sheet.[6] Low preparation temperatures (less than 700 K) have been attempted by many researchers. Although these do not usually result in perfect closed-shell structures, interesting nano architectures do arise.

For example, Leist et al.[7] showed that a number of different ammonium thiomolybdates could be decomposed by heating in sealed quartz tubes, and in dynamic vacuum (up to 673 K) resulting in onion like lamellae of MoS_2, but with open edges. It was also noted that the precursor $(NH_4)_2Mo_3S_{13}{\cdot}xH_2O$ shows decomposition behavior that is distinct from that of other ammonium thiomolybdates, in that its conversion to MoS_2 is characterized by a sharp exotherm. The explanation provided for this was the topochemical nature of the reaction resulting from structural relations between precursor and product. Zelenski and Dorhout[8] used alumina membranes as templates to decompose various ammonium thiomolybdates and obtained tubular nanostructures comprising linked spheres of lamellar MoS_2. Bezhverkhy et al.[9] have prepared highly disperse MoS_2 from an aqueous, pH-adjusted solution of ammonium thiomolybdate and hydrazine. The hydrothermal reaction of MoO_3 and Na_2S in HCl at 533 K results in bent MoS_2 sheets with a high surface area.[10] Afanasiev et al.[11] studied the effect of the surfactant cetyltrimethylammonium chloride on the thermal decomposition of $(NH_4)MoS_4$ using a two-step reaction. They obtained single MoS_2 layers at intermediate reaction temperatures (∼723 K) with very high surface areas of about 210 m^2/g. Similar sheetlike structures have been obtained by Peng et al.[12] by the reductive hydrothermal

* Authors to whom correspondence should be addressed. R.S. E-mail: seshadri@mrl.ucsb.edu. Fax: (805) 893 8797. W.T. E-mail: tremel@mail.uni-mainz.de.
[†] Johannes Gutenberg Universität, Mainz.
[‡] University of California Santa Barbara.

(1) Divigalpitiya, W. M. R.; Frindt R. F.; Morrison, S. R. *Science* **1989**, *246*, 369.
(2) Iijima, S. *Nature* **1991**, *354*, 56.
(3) Ugarte, D. *Nature* **1992**, *359*, 707.
(4) Tenne, R.; Margulis, L.; Genut, M.; Hodes, G. *Nature* **1992**, *360*, 444. Feldman, Y.; Wasserman, E.; Srolovitz, D. A.; Tenne, R. *Science* **1995**, *267*, 222.
(5) Rao, C. N. R.; Nath, M. *J. Chem. Soc., Dalton Trans.* **2003**, 1.
(6) Tenne, R. *Adv. Mater.* **1995**, *7*, 965.
(7) Leist, A.; Stauf, S.; Löken, S.; Finckh, E. W.; Lüdtke, S.; Unger, K. K.; Assenmacher, W.; Mader, W.; Tremel, W. *J. Mater. Chem.* **1998**, *8*, 241.
(8) Zelenski, C. M.; Dorhout, P. K. *J. Am. Chem. Soc.* **1998**, *120*, 734.
(9) Bezhverkhy, I.; Afanasiev, P.; Lacroix, M. *Inorg. Chem.* **2000**, *39*, 4516.
(10) Li, W.-J.; Shi, E.-W.; Ko, J.-M.; Chen, Z.-z.; Ogino, H.; Fukuda, T. *J. Cryst. Growth* **2003**, *250*, 418.
(11) Afanasiev, P.; Xia, G.-F.; Berhault, G.; Jouguet, B.; Lacroix, M. *Chem. Mater.* **1999**, *11*, 3216.

10.1021/cm0311170 CCC: $25.00
Published on Web 10/23/2003

reaction of molybdates with sulfur between 423 and 453 K. Iwata et al.[13] have prepared MoS_2 hydrogenation and hydrodesulfurization catalysts by thermal decomposition of ammonium thiomolybdate under 10% H_2S-H_2.

It is of interest to be able to prepare lamellar MoS_2 nanostructures in organic solvents, because of the ease of incorporation of structure-directing template molecules and surfactants. Surfactant molecules are well-known in their ability to control crystallite morphology, and in rare cases, the aggregation of crystallites.[14] Using solvothermal toluene as a reaction medium allows relatively high temperatures (required for crystallization) to be easily achieved, in an inexpensive and relatively nontoxic solvent. In the presence of capping agents, solvothermal toluene can be used to prepare oxide and chalcogenide nanoparticles, either through direct reaction or through decomposition of precursors.[15]

We present here our results on the use of solvothermal toluene at 653 K to decompose the thiomolybdate precursor, $(NH_4)_2Mo_3S_{13}\cdot xH_2O$, in the absence and presence of the surfactant cetyltrimethylammonium bromide (CTAB). We have employed novel and inexpensive means of obtaining the solvothermal conditions using a simple Swagelok-based autoclave. The samples have been characterized by X-ray diffraction in conjunction with DIFFaX simulations,[16] by transmission electron microscopy, and by surface area measurements. These studies indeed reflect the distinct natures of the products obtained by solvothermal decomposition as opposed to decompositions in static vacuum. The influence of the surfactant is also clearly manifested.

Experimental Section

The $(NH_4)_2Mo_3S_{13}\cdot xH_2O$ precursor was prepared as described in the literature[17] with some modifications as suggested by Leist.[18] Saturated $(NH_4)_2S_x$ (ammonium polysulfide) solution was prepared by bubbling a moderate flow of H_2S through a suspension of 80 g of sulfur in 400 cm^3 of 10% NH_3 solution for 3 h. The exothermic reaction yielded a dark red solution which was prepared just before being used, and filtered to remove unreacted sulfur and polysulfide precipitates. A 240 cm^3 aliquot of $(NH_4)_2S_x$ solution was then added to a solution of 8 g of $(NH_4)_6(Mo_7O_{24})\cdot 4H_2O$ in 40 cm^3 of H_2O, and the mixture was heated under reflux for 3 days at 363−373 K. The warm solution was filtered and the precipitated product was washed thoroughly with a $(NH_4)_2S_x$ solution, H_2O, CS_2, and EtOH (in that order), and then dried under vacuum. Identity was confirmed from the powder X-ray diffraction (XRD) pattern acquired on a Bruker D5000 diffractometer (Cu Kα radiation, 40 kV, 40 mA, transmission Bragg−Brentano geometry).

In this paper we compare results from two different synthetic routes. Preliminary experiments suggested that the precursor $(NH_4)_2Mo_3S_{13}\cdot x\ H_2O$ could be decomposed by heating at temperatures as low as 653 K for 24 h in a static vacuum (sealed quartz tube). Samples were therefore prepared by decomposing the precursor by heating at 653 K for 1 day, using the following conditions: (i) A sealed quartz tube. 300 mg of precursor was placed in an evacuated sealed quartz tube (10−12 cm long, 7 and 9 mm i.d. and o.d., respectively) and heated in a Thermolyne 1300 furnace. This sample is henceforth referred to as **Q**. (ii) Solvothermal preparation. 300 mg of precursor taken in 3 cm^3 of toluene (EM Science, 99.5%+, GR ACS) was heated in a sealed autoclave of 10 cm total volume. The autoclave comprised an SS316 tube, about 17 cm in length and 0.3″ i.d. and 0.5″ o.d., respectively, with the ends closed by Swagelok caps made from SS316 (SS-810-C, 0.5 in.). This sample is referred to as **S**. (iii) Preparations with surfactant. To the solvothermal preparation described above, 50 mg of CTAB was added before sealing the autoclave. This sample is referred to as **C**. In one case, 300 mg of CTAB was used. All the **C** samples were thoroughly washed between 5 and 10 times, each time with 50 mL of 2-propanol. After the last wash, the samples were dried at 343 K in air.

Caution: Heating the closed autoclave results very high autogenous pressure build up. It is important to use relatively small filling fractions in the autoclave (here approximately 30 volume %). The autoclaves were heated by placing them in a cold Thermolyne furnace that in turn was placed in an explosion proof cabinet. The furnace was equipped with an external (outside the cabinet) temperature controller. The cabinet was not opened when the furnace temperature was above 373 K.

The products of decomposition were characterized by XRD on a Scintag-X2 diffractometer (Cu Kα, 45 kV, 35 mA) operated in reflection Bragg−Brentano geometry, and by transmission electron microscopy (TEM) on a JEOL 2000 (200 kV acceleration voltage) equipped with energy-dispersive X-ray spectroscopy (EDS). Samples for TEM were prepared by depositing drops of an ethanolic suspension of the decomposition products (obtained by sonication) onto carbon-coated copper grids. Thermogravimetry analysis (TGA) was performed on a Mettler Toledo TGA/SDTA 851e, and BET specific surface area measurements were made on a Micromeritics ASAP2000 with N_2 as adsorption gas. Samples for surface area measurements were first treated by heating for 2 h at 623 K under N_2 purge on a Micromeritics FlowPrep060, followed by vacuum degassing overnight on the ASAP2000 at 623 K.

For each of the different preparation conditions several samples were prepared, and their powder XRD patterns recorded as a means of ensuring reproducibility of the preparation conditions.

Results and Discussion

Figure 1 displays powder XRD patterns of the products obtained from the three different routes described above, as well as a Rietveld simulation[19] of the powder XRD profile of crystalline 2*H*-MoS_2. Profile parameters used in the Rietveld simulation corresponded to those typically obtained from the specific diffractometer. In all cases 2*H*-MoS_2 (JCPDS Card 37-1492) was obtained. The patterns from the three samples show broadening of the peaks, which is typical for nanostructured phases, as well as the sawtooth patterns characteristic of layered disordered materials.[20] The solvothermal products (**S** and **C**) display patterns which are quite distinct from the product obtained after decomposition of the precursor in a sealed quartz tube. Notably, the (002) reflection at about 13° (2θ) is much less pronounced in

(12) Peng, Y.; Meng, Z.; Zhong, C. H.; Lu, J.; Yu, W.; Jia, Y.; Qian, Y. *Chem. Lett.* **2001**, 772.

(13) Iwata, Y.; Sato. K.; Yoneda, T.; Miki, Y.; Sugimoto, Y.; Nishyima, A.; Shimada, H. *Catal. Today* **1998**, *45*, 353.

(14) Li, M.; Schnablegger, H.; Mann, S. *Nature* **1999**, *402*, 393.

(15) Gautam, U. K.; Rajamathi, M.; Meldrum, F.; Morgan, P.; Seshadri, R. *J. Chem. Soc. Chem. Commun.* **2001**, 629. Thimmaiah, S.; Rajamathi, M.; Singh, N.; Bera, P.; Meldrum, F. C.; Chandrasekhar, N.; Seshadri, R. *J. Mater. Chem.* **2001**, *11*, 3215. Rajamathi, M.; Seshadri, R. *Curr. Opin. Solid State Mater. Sci.* **2002**, *6*, 337.

(16) Treacy, M. M. J.; Deem, M. W. *Computer code DIFFaX v. 1.803*, 1996. Treacy, M. M. J.; Newsam, J. M.; Deem, M. W. *Proc. R. Soc. London A* **1991**, *433*, 499.

(17) Müller, A.; Bhattacharyya, R. G.; Pfefferkorn, B. *Chem. Ber.* **1979**, *112*, 778.

(18) Leist, A., Thesis, University of Mainz, Germany, 1996.

(19) Rietveld simulation of the X-ray powder diffraction pattern of crystalline 2*H*-MoS_2 made use of the known crystal structure and the XND Rietveld code: Bérar, J.-F.; Garnier, P. *NIST Special Publication* **1992**, *846*, 212; Freely available from the CCP14 website at http://www.ccp14.ac.uk.

(20) Warren, B. E. *Phys. Rev.* **1941**, *59*, 693.

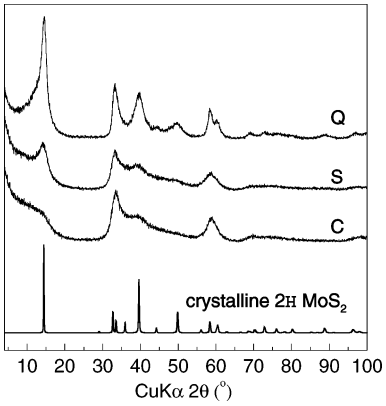

Figure 1. Powder X-ray diffraction patterns of the product obtained from decomposition of $(NH_4)_2Mo_3S_{13}{\cdot}xH_2O$ at 653 K for 24 h in an evacuated, sealed quartz tube (**Q**), in toluene (**S**), and in toluene in the presence of CTAB (**C**). A simulated XRD pattern of crystalline 2*H*-MoS_2 is also displayed.

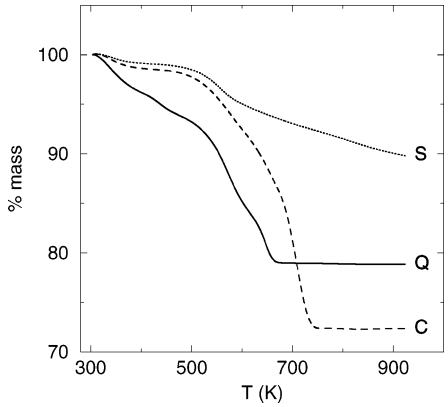

Figure 2. Thermogravimetric traces under flowing N_2 of the products **Q**, **S**, and **C**.

S and has almost no intensity in **C**. A more detailed analysis of the nanostructures based on DIFFaX simulations of powder XRD patterns is presented in the following sections.

Figure 2 shows thermogravimetric traces (in N_2) of the three MoS_2 products **Q**, **S**, and **C**. The product from the sealed quartz tube reaction (**Q**) has a large mass loss that we ascribe to adsorbed sulfur. We believe this because, for this sample, the purging and degassing associated with the BET surface area measurements resulted in yellow sulfur deposits on the walls of the vial. Such deposits were not observed for the other samples. It is possible that in static vacuum, there is no process of cleaning the high-surface-area MoS_2 that is formed, unlike in the solvothermal preparations where the samples are "washed" by the solvent during preparation. The mass loss of the solvothermally prepared sample is associated with small amounts of absorbed matter (perhaps products of the decomposition of the precursor) and indeed, the extent of the mass loss is the smallest in this sample. The sample prepared in the presence of CTAB (**C**) shows the largest mass loss (about 27 mass %). Till nearly 580 K, the mass loss in sample **C** is quite similar to that for **S**, and perhaps corresponds to adsorbed material. After this temperature, there is a sharper fall in mass that corresponds to the CTAB adsorbed in the sample being stripped off. This CTAB that was not removed by the extensive washing is intrinsic to the nanostructure. However,

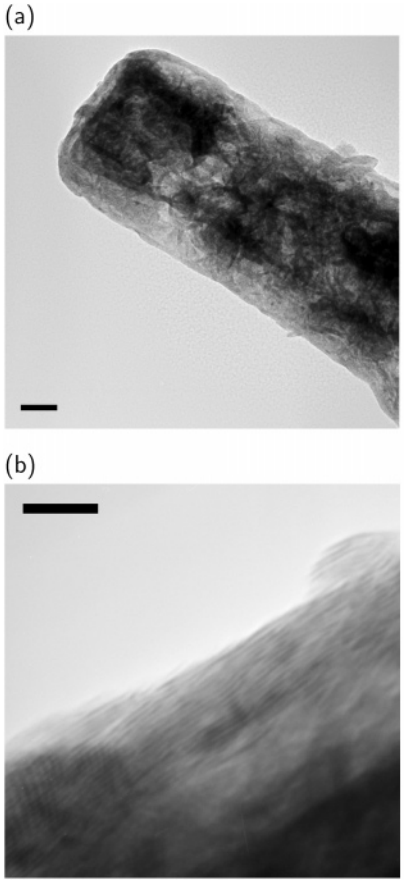

Figure 3. TEM images of the product **Q**. The scale bars are (a) 50 nm and (b) 10 nm.

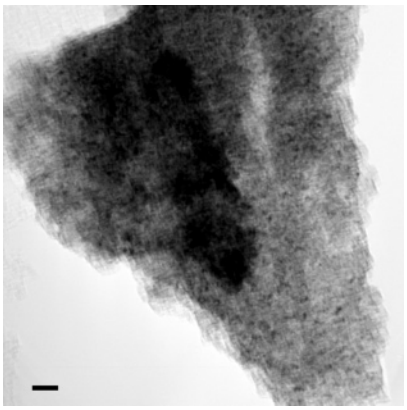

Figure 4. TEM image of the product **S**. The scale bar is 20 nm.

CTAB could not be detected in EDS analysis of the **C** sample.

Transmission electron micrographs of the different decomposition products are displayed in Figures 3, 4, and 5. The samples obtained from sealed-tube decompositions (**Q**) retain the needlelike morphology (Figure 3(a)) of the starting material for which scanning electron microscope images have been previously presented.[7] A closer examination at high magnification reveals characteristic MoS_2 lamellae, with sheets separated by about 7 Å.

The sample obtained by solvothermal decomposition in pure toluene (Figure 4) is seen to be quite distinct from **Q**. The morphology does not display the needlelike shapes seen for the **Q** sample, but instead displays

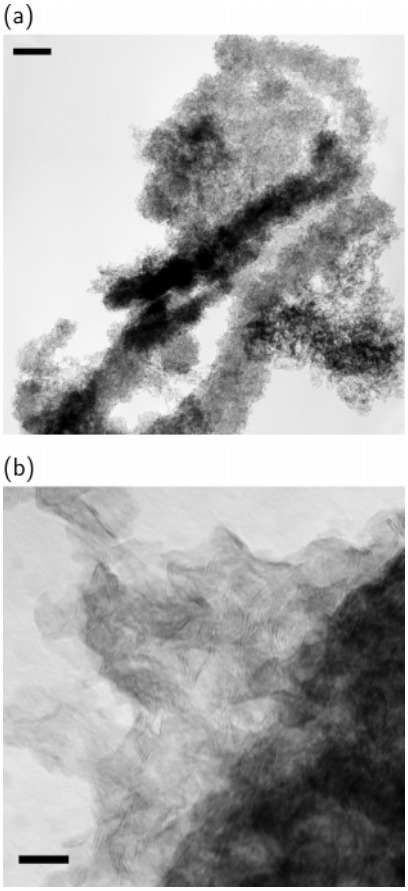

Figure 5. TEM images of the product **C**. The scale bars are (a) 100 nm and (b) 10 nm.

isotropic agglomerates. Toward the edges of the agglomerate, the sheetlike nature of the constituent MoS_2 becomes apparent.

When the surfactant CTAB is added to the solvothermal preparation, we once again observe in the TEM that the morphologies of the MoS_2 so formed (**C**) are quite distinct from what is obtained from the sealed-quartz tube decomposition (**Q**). Some portions of the **C** samples that we studied by TEM resembled images that were obtained from the **S** sample. In addition, certain regions of the TEM grid displayed string-like structures (Figure 5(a)). We propose that aggregation of surfactant molecules is responsible for the formation of such unusual morphologies. Seen in higher magnification (Figure 5(b)), the **C** sample shows bent MoS_2 lamellae with interlayer spacing of about 7 Å. Whereas in **Q** the regions of stacked sheets were up to 100 nm long with stacking perpendicular to the needle surface, these regions are significantly shorter for **C** and their orientation is completely at random with respect to other similar stackings. TEM studies, while providing details of morphology, can be unsatisfactory in terms of how representative they are with respect to the entire sample. To arrive at a quantitative description of the different MoS_2 samples, we have used the DIFFaX program[16] to generate different stackings of individual MoS_2 lamellae and simulated powder X-ray diffraction patterns from the structures so obtained. Many series of DIFFaX simulations were carried out, varying the in-plane extent of the layer, the number of layers, and finally the proportion of faulted stackings (e.g., stackings that ignore orientational relationships between layers)

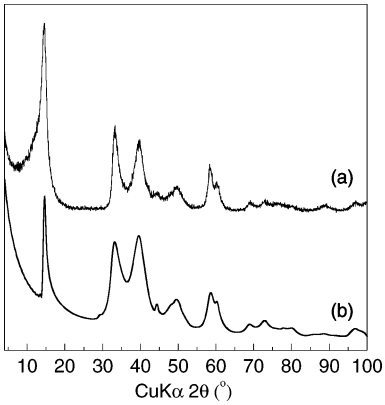

Figure 6. Powder X-ray diffraction patterns of (a) the product **Q** and (b) DIFFaX simulation of 20 layers of MoS_2, each 10 × 10 nm on side and using a probability of 60% random stacking.

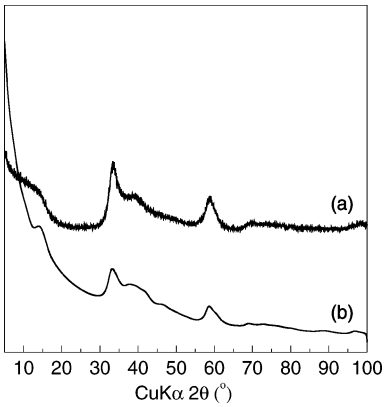

Figure 7. Powder X-ray diffraction patterns of (a) the product **C** and (b) DIFFaX simulation of 5 layers of MoS_2, each 10 × 10 nm in size stacked in a completely random manner.

to the simple ABAB stacking of crystalline 2*H*-MoS_2. Those that matched most closely (visual comparison) with the corresponding experimental X-ray diffraction patterns are displayed in Figure 6 (for **Q**) and Figure 7 (for **C**). Each DIFFaX simulation is time-consuming and the nature of the parameters that can be varied does not permit the program to be used as a "best-fit" tool.

By choosing 20 layers with a rather small layer (in-plane) size of (10 × 10 nm) and a probability of 60% completely random stacking, we could obtain a simulated pattern which showed the characteristics of the **Q** experimental XRD pattern: the relatively sharp and intense (002) peak corresponding to the number of layers, and the sawtooth peak shape resulting from the stacking disorder. Random stacking was necessary to obtain the correct relative intensities. It also contributed to the peak broadening, and the peak shape. To simulate the **C** experimental pattern far fewer than five layers with the same in-plane size (10 × 10 nm), as well as completely random stacking of the MoS_2 layers, were required for the simulation to correspond to what was observed experimentally. This is in agreement with TEM results. TEM images suggest a larger in-plane size for the **Q** sample when compared with the **C** sample. The suitability of using the same in-plane size (10 × 10 nm) for both sets of simulations can perhaps be reconciled as follows: X-ray diffraction is sensitive to crystalline correlations, whereas TEM images are a physical representation of the electron density. It is possible that the (larger) sheets observed in the TEM image of the **Q**

Table 1. Surface Areas and Median Pore Diameters Obtained from N_2 Adsorption Measurements

			C[a]	
	Q	**S**	(6:1)	(1:1)
surface area (m^2/g)[b]	77.7	52.6	152.9	175.3
median pore diameter (Å)[c]	8.1	8.2	7.7	7.5

[a] Two samples prepared with different starting mass ratios of $(NH_4)_2Mo_3S_{13}\cdot xH_2O$ to CTAB were prepared for BET measurements as indicated (6:1 and 1:1). [b] Determined using the BET method. [c] Determined using the Horvath−Kawazoe method.

sample are defective, with small X-ray correlation lengths.

We note that the sharp rise in the low-angle regions of the experimental powder XRD patterns is not easily modeled by the DIFFaX simulation. In the experiment, it corresponds to scattering from a collection of small particles (as opposed to a perfect crystal which would not scatter at $2\theta = 0$). DIFFaX does not account for low-angle scattering that arises from a collection of particles.

The consequences of the different nanostructurings manifest as rather different surface areas. The results of BET surface area measurements are summarized in Table 1. All samples display relatively high surface areas (>50 m^2/g). The values for the product from sealed quartz tube reactions are slightly higher (77.7 m^2/g) than previously reported (max. 64.4 m^2/g) for this method.[7] The solvothermal method without surfactant does not increase the surface area, but introducing CTAB with the precursor significantly increases the BET specific surface areas (152.9 m^2/g).

The median pore diameter determined by the Horvath−Kawazoe method is similar for all products, being about 8 Å.

Conclusions

We have presented here a one-step, low-temperature method to obtain high-surface-area nanostructured MoS_2 by using solvothermal conditions. The presence of the surfactant CTAB was crucial to obtaining the interesting string-like morphology of the product MoS_2 as well as high surface areas. The distinct nature of the product prepared in the presence of the surfactant has been confirmed by TEM, BET, and TG analysis, and XRD in conjunction with DIFFaX simulations.

Acknowledgment. This work made use of MRL Central Facilities supported by the National Science Foundation under award DMR 96-32716. The *Deutsche Akademische Austauch Dienst* is gratefully acknowledged for a short-term Graduate Student fellowship to N.B., supporting her visit to UCSB. This work was partially supported by the MRL program of the National Science Foundation under Award DMR00-80034. R.S. acknowledges a start-up grant from the Dean, College of Engineering, UCSB. N.B., T.G., and W.T. thank the BMBF (Support 03N6500) for financial support of their work in Mainz.

CM0311170